Early Frasnian (Upper Devonian) Genundewa event in the Bolshaya Nadota river section of the Sub-Polar Urals (Russia)

Marina SOBOLEVA[1], Denis GRUZDEV[1], Dmitriy SOBOLEV[1], Andrey ZHURAVLEV[1]

[1]Institute of Geology of Komi Science Centre of the Ural Branch of the Russian Academy of Sciences, Syktyvkar, Russia

*Correspondence: matusha.888@mail.ru

ORCIDs:

First AUTHOR: https://orcid.org/0009-0001-4904-8107

Second AUTHOR: https://orcid.org/0000-0002-6100-7148

Third AUTHOR: https://orcid.org/0000-0001-7097-2874

Forth AUTHOR: https://orcid.org/0000-0003-4043-6303

Abstract: Evidence of the Frasnian Genundewa Event in the FZ 2 – FZ 3 boundary interval was detected in the facies of the isolated carbonate platform in Sub-Polar Urals. The preserved traces of the Genundewa Event represent micritic microlaminated carbonates, which manifests the short-term deepening episode on the extremely shallow water background. From the onset of this deep-water deposition there is a dominance of *Polygnathus*, *Ancyrodella*, and *Mesotaxis* whereas in the underlying shallow-water deposits the genus *Polygnathus* clearly predominated. No specific features of the Genundewa event in the C-isotope record were observed. The mean $\delta^{13}C_{carb}$ value is about 2‰ in the event interval. The onset of the Genundewa Event corresponds to the beginning of Euro-American IIb2 cycle and is correlated with the base of the

Sargaevian regional substage of the Urals and Russian Platform and the base of Poland IC cycle, which confirms the global character of this event.

Key words: Genundewa Event, Upper Devonian, Frasnian, conodonts, Sub-Polar Urals, Matyashor Formation.

1. Introduction

The Frasnian was a time of numerous events of different scale and nature (e.g. Johnson et al., 1985; Sandberg et al., 1988; Walliser, 1996; House, 2002; Racki, 2005; Becker et al., 2016, 2020; Pisarzowska et al., 2020). Some of these events have been studied in detail (e.g. Frasne, Middlesex, Semichatovae, and Kellwasser events), but some others have received less attention, especially in the NW Laurussia region. One of the understudied events is the Genundewa Event, first proposed in North America by M.R. House and W.T. Kirchgasser (1993). This event is based on the dual maximum transgression of the Genundewa Limestone in New York, near the FZ 2 – FZ 3 boundary. Becker et al. (2016) classified the event as a secondary event in terms of the degree of eustatic manifestation and change in biota. The work of House (2002) interpreted the Genundewa Event as anoxic facies of pelagic stylyolinites with poor benthos. Another feature of this event is a deepening when the source of the sedimentary material was substantially removed. This contributed to sedimentary starvation (House and Kirchgasser, 1993).

The transgressive Genundewa Event contributed to the spread of deepening environments that spanned North America (House and Kirchgasser, 1993), Central Poland (Racki, 1993), South Timan (House et al., 2000; Sobolev et al., 2023), the

Subpolar Urals, Russia (Soboleva et al., 2018a) and Western Australia (Becker and House, 1997). In most cases, the transgression is well recorded in pelagic ammonoid and stylyolinite dominated facies which are often anoxic. In shallow-shelf environments, traces of this event are rarely preserved due to erosion during the subsequent regression. The Genundewa transgression plays an important role in global correlation and comparison of different facies. Its start coincides with North America IIb-2 cycle (Johnson et al., 1985; Day et al., 1996; Day, 1998). In the Russian Platform and the Urals, the beginning of the event coincides with the base of a major sedimentation cycle (Rodionova et al., 1995; Tikhomirov, 1995) that accounts for the largest area of marine sediment spreading in the Devonian time in NE Laurussia.

In the Sub-Polar Urals, Russia, studies associated with the Genundewa Event have focused on an isolated carbonate platform of the shelf edge environments. In order to recognize it, this study focuses on the high-resolution conodont biostratigraphy, micro-facies analysis, and carbon isotopic record of the Frasnian Matyashor Formation on the Bolshaya Nadota river in the Olysya Mountain area.

The slow and uneven subsidence of the shelf margin, where the isolated carbonate platform was located, resulted in punctuated sedimentation with numerous gaps in the sedimentary sequence (Gruzdev, 2021). Therefore, the traces of global events in the sequences of this facies belt are poorly known and the peculiarities of the manifestation of the events are hardly studied. The studied section represents a unique opportunity to study the manifestation of the Genundewa Event in the isolated carbonate platform facies.

2. Genundewa Limestone in type region

The Genundewa Limestone is a distinctive and widespread mass accumulation of styliolines in the mid-Genesee Group between the Penn Yan Shale and West River Shale in western New York. The Genesee Group succession represents deposition in dysoxic to near anoxic settings in the subsiding Appalachian foreland basin (Baird et al., 2006). The following divisions are identified in the type area: Lower Genundewa Limestone, North Evans Limestone and Upper Genundewa Limestone (House and Kirchgasser, 1993; Baird et al., 2006; Klapper and Kirchgasser, 2016). The Lower Genundewa Limestone lies with a break on the black shales of the Penn Yan Formation and is represented by stylioline packstone-grainstone (15-23 cm) with abundant goniatites and the Frasnian Zone 2 conodont *Ancyrodella rotundiloba* (Bryant). The North Evans Limestone (= "Conodont-bed" of Hinde, 1879) overlayed the Lower Genundewa Limestone or, with a gap, the black shales of the Penn Yan Formation or older strata. These deposits are represented by crinoid subfacies 10-15 cm thick or bone subfacies rich in detrital pyrite in the lower first few centimetres. The North Evans Bed often contains large quantities of redeposited conodonts, reworked limestone nodules and glauconite grains typical of a lag deposit. The age of the North Evans Limestone corresponds to FZ 2 (Baird et al., 2006).

The Upper Genundewa Limestone is generally massive, 18-40 cm thick. It is composed of dark gray stylioline grainsnone-packstone. In some sections in the type area, a bed of black mudstones 15-25 cm thick is located at the base of the Upper Genundewa, which lies on the North Evans Limestone. The Upper Genundewa Limestone contains the Frasnian Zone 3 conodonts *Ancyrodella recta* Kralick, *Ad. triangulata* Kralick and *Ad. rugosa* Branson and Mehl (Kralick, 1994; Klapper and Kirchgasser, 2016).

The Genundewa transgressive event thus comprises a narrow stratigraphic interval in the type area, where the boundary of FZ2 and FZ3 is recognized. Distinct conodont faunas are recognized in the Lower and Upper Genundewa Limestone by the presence of certain *Ancyrodella* species (Kralick, 1994; Klapper and Kirchgasser, 2016).

House and Kirchgasser (1993) believed the Genundewa Limestone of New York to have the closest faunal and facial affinities to the Squaw Bay Limestone of Michigan. The Squaw Bay Limestone represents the uppermost unit of the Traverse Group. The Traverse Group is overlain by the Antrim Shale, which represents a major tectonic event in the Michigan Basin and Appalachian region. The result was the deposition of vast quantities of black mud into the Michigan Basin from the Appalachian highlands (Kimmel, 1973). Characteristic fossils in Squaw Bay Limestone include goniatite cephalopods, *Styliolina*, and conodonts of FZ 2 - FZ 3 (Müller and Clark, 1967).

3. Geological settings

Olysya Mountain is a complex geological area containing terrigenous as well as bioherm and reef carbonate formations of Lower Devonian to Lower Permian ages with sharp facies transitions. The Nadotamylk Formation (Lower to Middle Devonian), Matyashor Formation (Middle to Upper Devonian), Bolshaya Nadota Formation (Upper Devonian to Lower Carboniferous), combined limestone-dolomite and limestone-breccia formations (Lower Carboniferous), Olysya Reef Massif (Lower Carboniferous), and Lower Permian deposits are recognized in the area (Sobolev et al., 2000). Figure 1 shows the panoramic view of the Devonian-Carboniferous succession.

The foundations of regional geology, tectonics and stratigraphy of the Olysya Mountain area were laid by Voinovsky-Kriger (1945), Raaben (1959), Eliseev (1978),

Puchkov (1979), Shishkin (1989, 1999). Sobolev et al. (2000) proposed a detailed geological map and stratigraphic scheme for this area. A model for the formation of the Devonian-Carboniferous deposits in the study area is presented in the papers of Skompski et al. (2001) and Gruzdev (2017, 2021). At the beginning of the Frasnian, an isolated carbonate platform formed in the Subpolar Urals, bounded to the west by the Kozhim intra-shelf depression and to the east by the Ural paleobasin (Gruzdev et al., 2016; Gruzdev, 2017, 2021). The emerging landscape system is characterized by the development of shoals and organogenic buildups of an isolated carbonate platform (Gruzdev, 2017).

According to Sobolev et al. (2000), Skompski et al. (2001), Zhuravlev (2002), Gruzdev and Zhuravlev (2003) and Gruzdev et al. (2016), the Olysya Mountain is formed by organogenic buildups of different ages combined along the thrusts. The Late Viséan-Serpukhovian deposits compose the upper part of Olysya Mountain. The lower part of Olysya Mountain consists of the Frasnian carbonate deposits of the Matyashor Formation. The Matyashor Formation in the Bolshaya Nadota river section consists of massive microbial-algal limestones, forming 3-5 meters thick bioherms, and bioclastic limestones, with a massive or lenticular-layered structure.

The Bolshaya Nadota river section (Outcrop Nd8; 65°39′38″ N, 60°58′04″ E) is located in the Subpolar Urals, about 46 km southeast of the Inta (Russia) railway station (Figures 2A). Structurally, the area occupies the western part of the Ural folded-thrust belt and belongs to the West Ural structural zone bounded in the west by the Pre-Ural foredeep along the West Ural Main Thrust (Figure 2B) and in the east by the Lemva allochthon (Figure 2C), which consists of a series of tectonic sheets (Yudin, 1994;

Timonin, 1998). The studied section is located in the frontal zone of the Lemva allochthon and is complicated by faults and thrusts (Figures 2C).

4. Material and methods

The material for this investigation was collected in the Bolshaya Nadota river section in 1999-2003 and published in a series of articles (Sobolev et al., 2000; Zhuravlev, 2002, 2012; Gruzdev and Zhuravlev, 2003; Gruzdev et al., 2016; Gruzdev, 2017, 2021). Some of the samples were recently processed in 2020-2022. The biostratigraphic subdivision of the Bolshaya Nadota river section is now more detailed (Figure 2D). Conodonts provide a biostratigraphic framework for the studied section. Conodont elements were found in 21 samples and are represented by *Ancyrognathus (Ag)*, *Ancyrodella (Ad)*, *Belodella (B)*, *Icriodus (I)*, *Mehlina (Me)*, *Mesotaxis (M)*, *Palmatolepis (Pa)*, *Polygnathus (P)*, *Schmidthognathus (S)*, *Youngquistognathus (Y)*, and *Zieglerina (Z)*. Abbreviations of genera are given in parentheses.

Figure 3 shows the general view of the Frasnian Matyashor Formation. A total of 32 samples were collected from the 36 m interval covering this deposits. Conodont samples were dissolved in 10% buffered acetic acid. The residues were washed through a 70 μm sieve, dried and the conodont elements were extracted. A binocular microscope was used for the picking and the determination of the specimens. A total of 723 conodonts were identified. The conodont elements obtained from the Bolshaya Nadota river section are well preserved and have a conodont colour alteration index (CAI) between 4.0 and 4.5. The conodonts were photographed using a Tescan Vega 3 LMH scanning electron microscope. The collection of conodonts is stored in the A.A. Chernov

Geological Museum of the Institute of Geology, coll. no. 492/18-26 (Syktyvkar, Russia).

Thin sections were made of each sample to study microfacies (MF). The sedimentological classification of the carbonates follows Dunham (1962). Four types of microfacies have been identified in the section: MF-1 is represented by wackestones, MF-2 by packstones, MF-3 by floatstones, and MF-4 by framestones. The limestones are recrystallized to varying degrees, which greatly complicates the interpretation of the primary facies of the sediments.

The bulk-rock samples for the isotope analysis were collected from fresh limestones with average stratigraphical spacing of meters. The samples are distributed as following: 10 samples from the *M. falsiovalis* Zone (= FZ 1 – FZ 3), 3 samples from the *Pa. transitans* Zone (= FZ 4), 3 samples from the *Pa. punctata* Zone (= FZ 5), and 7 samples from the *Pa. jamieae* - Lower *Pa. rhenana* zonal interval (= FZ 11 – FZ 13a). A total of 24 samples were analyzed for carbon and oxygen stable isotopes.

Carbonate powder for isotope analysis was extracted from fresh surfaces of rock samples using a steel microdrill. The carbon and oxygen isotope composition of the carbonates was studied with a DELTA V Advantage mass spectrometer with sample preparation on a Gas Bench II line by standard methods. $\delta^{13}C_{carb}$ values were reported relative to the Vienna Pee Dee Belemnite (VPDB) standard and $\delta^{18}O_{carb}$ values were reported relative to the Standard Mean Ocean Water (SMOW) standard. The precision of the $\delta^{13}C_{carb}$ value is ±0.04‰ and precision of the $\delta^{18}O_{carb}$ value is ±0.06‰. Isotope analysis was performed at the CKP “Geonauka” of the N.P. Yushkin Institute of Geology Komi SC UrB RAS (Syktyvkar, Russia). Statistical methods were performed

using the PAST software (Hammer et al., 2001). Two screening tests were used for evaluating the reliability of the isotope record (Zhuravlev et al., 2020):

1. Visual examination of the samples. Fresh surfaces of samples were used to drilling out the carbonate powder for analyses.

2. Distribution of carbon and oxygen stable isotopes. A composite screening diagram (Zhuravlev et al., 2020) was used. Samples located in the doubtful area of the diagram were excluded from the following analyses. All the studied samples excluding БН8-177 passed the screening tests.

5. Results

5.1. Description of studied section

The succession of the studied section is subdivided into members based on the field lithological description and microfacies analysis (Figures 4 and 5).

1. Gray to dark gray limestones with a massive structure (packstone). In the lower part of the member, the limestone is coarse-grained with lithoclasts of peloidal limestone and organogenic debris (Sample 1). The fauna is represented by fragments of brachiopods and crinoids. In the upper part of the member - medium-coarse detrital limestones with micrite, peloid and finely detrital bulk (Sample 2). The fauna is represented by fragments of brachiopods and conodonts. Incomplete member thickness 0.7 meters.

2. Gray to dark gray limestones with a massive structure (floatstone). The unsorted and angular fragments are composed of algal (nodules and crusts) light gray limestones. The cement is microfine grained. Rocks contain fragments of brachiopods, crinoids, algae,

corals. Rare conodonts and thick-walled ostracod shells occur (Sample N4-2/99). Member thickness 1.9 meters.

3a. Gray to dark gray limestones with a massive structure (floatstone). In the lower part of Member 3a they are rare semi-rolled fragments (up to 3 mm) of micritic limestone (Sample 4). In the upper part of the member the fragments are composed of subrounded and rounded microbial-algal limestones (Sample БН8-258). The fauna is represented by fragments of brachiopods, crinoids, algae and conodonts (Sample 4). Member thickness 3.6 meters.

3b. Light to dark gray colored microlaminated limestones (wackestone). The texture is fine to medium grained with rounded rare fragments of micritic limestone (Sample 5/3). Some layers are substantially recrystallized. The fauna is represented by conodonts, rare whole shells of thin – walled ostracods and brachiopods (up to 2-3 mm). Member thickness 2.2 meters.

4. Gray limestones with a massive structure (floatstone). Coral fragments larger than 2 mm can be found among the formational elements. The matrix is micritic. The rocks are partly dolomitized. The bioclastic material is represented by the remains of algae, corals, crinoids, brachiopods, and conodonts (Sample 7). Member thickness 0.4 meters.

5. Dark gray colored lens-like bedded limestones (wackestone). Rare fossils are represented by crinoids and brachiopods (Sample 8). There are rare remains of conodonts. Member thickness 0.2 meters.

6a. Gray limestones with a massive structure, algal textures with bioclasts (crinoids) and peloids are common (framestone). Member thickness 7.6 meters.

6b. Gray peloidal-detritic limestones with algal nodules and crusts and angular lithoclasts of bioclastic limestones (floatstone) (Sample 9/3). Member thickness 2.8 meters.

6c. Gray biomorphic limestones (framestone). Member thickness 3.0 meters.

A tectonic fragmentation zone is observed higher up. Thickness 2.0 meters.

7. Gray limestones with a massive structure, from fine to coarse grained (packstone). Rare lithoclasts (up to 5 mm) occur in the lower part of the member. Bioclasts are represented by crinoids. Member thickness 7.6 meters.

8. Gray limestones with a massive structure. The lower part of the member is coarse-grained limestone with rare oolites (packstone). Fossils are represented by echinoderms and brachiopods. In the upper part of the member, the limestones are indistinctly layered. The texture is fine to medium grained, partially recrystallized (wackestone). Incomplete member thickness 4.0 meters.

5.2. Microfacies

The microfacies identified in the Bolshaya Nadota river section were used as a basis for reconstructing the Frasnian environment in the area under consideration. Four microfacies (MF) types are recognized based on microscopic features, matrix, sedimentary textures, and fossil content (Figure 6).

MF-1. Wackestone.

Light to dark gray limestones, thin-bedded (3-5 cm thick) with microlamination (Figure 6-1). The texture is fine to medium grained with rare rounded intraclasts of micritic limestone. Organic remains are represented by conodonts, rare whole shells of thin-

walled ostracods and brachiopods up to 2-3 mm. The sediments were formed in calm-water conditions, below the wave base.

MF-2. Packstone.

Gray to dark gray color limestones with a massive structure. Lithoclasts and bioclasts greater than 2 mm are rare and represented by peloids and fine-detritic aggregates (Figure 6-2). The fauna is represented by fragments of brachiopods, crinoids, and conodonts. The sediments were formed in moderately active water conditions with periodic wave action.

MF-3. Floatstone.

Gray to dark gray color limestones with a massive structure. Formational elements range from 0.25 mm to 3-5 mm (Figure 6-3). Unsorted and angular lithoclasts are composed of light gray algal limestones. The cement is microfine grained. Bioclastic material is represented by brachiopods, crinoids, algae, and corals. Rare conodonts and thick-walled ostracod shells occur. The sediments were formed in calm-water conditions with periodic wave action on the bottom.

MF-4. Framestone.

Gray limestones with massive skeleton structure, organogenic (algal), and bioclastic. Algal textures with sandy admixtures of semi-coated lithoclasts, bioclasts (crinoids) and peloids are common. Microbial-algae limestones, with traces of growth of microbial communities forming characteristic patterned structures (Figure 6-4). The sediments occurred under moderately active water conditions, at the depth of the normal wave

base. In the absence of strong waves, the growth of attached and crusted organisms occurred.

Transitions from MF-2 to MF-3, MF-1 to MF-3, MF-1 to MF-4 and MF-3 to MF-4 are considered to be signs of regression. Transitions from MF-3 to MF-1, MF-4 to MF-3 and MF-2 to MF-1 are likely to represent transgression.

5.3. Conodont biostratigraphy

The conodonts of the Matyashor Formation were first studied by Zhuravlev (2002). The latest results of the conodont study were published by Gruzdev et al. (2016). The new data obtained allow refinement of the biostratigraphic subdivision of the section, especially in the lower part of the Matyashor Formation. All of our previously published conodont data are incorporated in this paper.

In this study, Standard Conodont Zonation (Ziegler and Sandberg, 1990) and Frasnian Zonation (Klapper, 1989; Klapper and Kirchgasser, 2016) are used as the biostratigraphic framework for the Matyashor Formation of the Bolshaya Nadota river section (Figure 2D). Conodont zones are indicated either by the First Occurrence Datum (FOD) of the index-species or by the presence of characteristic taxa. Due to a fault in the middle part of the section some successive conodont zones are missing from the biostratigraphic record. The distribution and numbers of conodonts found in the Matyashor Formation are shown in Table 1 and Figure 4, and characteristic forms are illustrated in Figures 7-11.

The base of the Bolshaya Nadota river section begins in FZ1. Sample 2 did yield the important conodonts *Ad. binodosa* Uyeno, *P. dubius* Hinde, *P. ljaschenkoi* Kuzmin, *P. pennatus* Hinde, and *Y. angustidiscus* (Youngquist). Other associated species are *I.*

expansus Branson and Mehl, *I. symmetricus* Branson and Mehl, *I. vitabilis* Nazarova, *P. decorosus* Stauffer, and *P. xylus* Stauffer. Conodonts *P. latifossatus* Wirth, *I. obliquimarginatus* Bischoff and Ziegler, *P. parawebbi* Chatterton, and *P. varcus* Stauffer found in samples 2 and N4-2 are characteristic of the Givetian (Table 1). It is possible that these conodonts survived until the Early Frasnian or were redeposited due to local tectonic movements of individual blocks within an isolated carbonate platform.

The previous position of *P. varcus* Stauffer was limited to the *P. varcus-S. hermanni* zones of the Givetian, however Aboussalam (2003) suggested that its last appearance is in the Middle Frasnian. The entry of *Ad. binodosa* Uyeno (= *Ad. rotundiloba* early form) in Sample 2 indicates the base of the Frasnian; this taxon also serves to recognise FZ 1 (Aboussalam and Becker, 2007). Index species *Ad. pristina* Khalymbadzha and Tchernysheva of the FZ 1 was not found in samples 2 and N4-2, but occurs later in Sample 3.

The FOD of *Ad. rotundiloba* (Bryant) in Sample 3 defines the base of FZ 2. Sample 3 is rich in diverse polygnathids, such as *P. alatus* Hiddle, *P. dengleri dengleri* Bischoff and Ziegler, *P. dengleri sagitta* Aboussalam and Becker, *P. dubius* Hinde, *P. foliatus* Bryant, *P. ljaschenkoi* Kuzmin, *P. pennatus* Hinde, *P. pollocki* Druce, *P. praepolitus* Kononova, Alekseev, Barskov and Reimers, *P. pseudoxylus* Kononova, Alekseev, Barskov and Reimers, *P. webbi* Stauffer, and *P. xylus* Stauffer. Most of the species have a long stratigraphic range from the Upper Givetian *Kl. disparilis* Zone to the Middle Frasnian FZ 6. Samples 3 to N4-5 can be assigned to FZ 2.

The base of FZ 3 was recognised by the FOD of *Ad. recta* Kralick in Sample 5/2, because this species appears at the same level as the index species *Ad. rugosa* Branson and Mehl (Kralick, 1994; Klapper et al., 2004; Klapper and Kirchgasser, 2016). The

index species *Ad. rugosa* Branson and Mehl of FZ 3 is absent in the study material. Other important associated species are *Ad. alata* Glenister and Klapper, *Ad. rotundiloba* (Bryant), *M. asymmetrica* Bischoff and Ziegler, *M. bogoslovskyi* Ovnatanova and Kuzmin, *M. falsiovalis* Sandberg, Ziegler and Bultynck, *Z. nuda* Bardashev and Bardasheva, and *Z. ovalis* Ziegler and Klapper. Icriodontids and polygnathids are rare. Typical specimens of *Ad. alata* Glenister and Klapper and *M. asymmetrica* Bischoff and Ziegler occurs in Sample 5/2 and Sample 6/1, respectively. Samples 5/2 to 6/2 can be correlated with FZ 3.

The FOD of *Pa. transitans* Müller in Sample 7 defines base of FZ 4 (Klapper and Kirchgasser, 2016). The conodont assemblage is extremely depleted in this interval. Other associated species are *I. symmetricus* Branson and Mehl, *M. asymmetrica* Bischoff and Ziegler, *M. falsiovalis* Sandberg, Ziegler and Bultynck, *P. decorosus* Stauffer, *P. pennatus* Hinde, *P. pollocki* Druce, and *Y. angustidiscus* Youngquist. Samples 7 to 9/2 can be correlated with FZ 4.

The base of FZ 5 was recognised by the occurrence of *P. timanicus* Ovnatanova in Sample 9/3, because this species has almost the same First Appearance Datum (FAD) as the index species *Pa. punctata* (Hinde) (Ovnatanova and Kononova, 2001; Pisarzowska et al., 2006, 2020; Soboleva et al., 2018a, 2018b) which is absent. Other associated species are *M. asymmetrica* Bischoff and Ziegler, *M. falsiovalis* Sandberg, Ziegler and Bultynck, *I. symmetricus* Branson and Mehl, *Pa. transitans* Müller, *P. lodinensis* Pölsler, *P. pseudoxylus* Kononova, Alekseev, Barskov and Reimers, *P. uchtensis* Ovnatanova and Kuzmin, *P. xylus* Stauffer, and *Z. ovalis* Ziegler and Klapper. *Polygnathus uchtensis* Ovnatanova and Kuzmin and *P. lodinensis* Pölsler are species mostly known from the *Pa. punctata – Pa. hassi* zonal interval, but probably originated

from the upper part of *Pa. transitans* Zone (Soboleva et al., 2018a). Due to a fault in the middle part of the studied section, the upper boundary of FZ 5 can not be traced.

The FZ 6 - FZ 10 are absent in the sequence for stratigraphic or tectonic reasons. Due to complete recrystallisation of this part of the section, conodonts in the carbonates (Sample 10 and Sample 11) were probably not preserved.

Samples 12 to 15/2 can be roughly correlated with the FZ 11 - FZ 12. This interval is rich in diverse palmatolepids. Ancyrodellids, icriodontids, and polygnathids are scarce. The base of FZ 11 was recognised by the FOD of *Pa. foliacea* Youngquist and *Pa. timanensis* Klapper, Kuzmin and Ovnatanova in Sample 12, because these species have almost the same FAD level as the index species *Pa. feisti* Klapper and *Pa. semichatovae* Ovnatanova (Klapper and Kirchgasser, 2016; Saupe and Becker, 2022). Other important associated species are represented by *Ancyrodella nodosa* Ulrich and Bassler, *Pa. amplificata* Klapper, Kuzmin and Ovnatanova, *Pa. hassi* Müller and Müller, and *Pa. lyaiolensis* Khruscheva and Kuzmin. Most species range into the overlying FZ 11b (Saupe and Becker, 2022). The index species *Pa. nasuta* Müller of the FZ 11b occure in Sample 14. Index species *Pa. winchelli* of the FZ 12 is absent in the study section. The important associated species that indicate of FZ 12 are represented by *Pa. brevis* Klapper, Kuzmin and Ovnatanova, *Pa. eureka* Ziegler and Sandberg, *Pa. foliacea* Youngquist, and *Pa. kozhimensis* Yudina. Most species are known mostly from the *Pa. jamieae* – *Pa. rhenana* zonal interval (Ziegler and Sandberg, 1990).

The FOD of *Pa. bogartensis* Stauffer in Sample 16 defines the base of FZ 13a (Klapper and Kirchgasser, 2016). *Palmatolepis bogartensis* Stauffer is a rare species in the Bolshaya Nadota river section.

The conodont biostratigraphy of the Bolshaya Nadota river section indicates that the Matyashor Formation ranges from the Frasnian Zone 1 to the FZ 13a with a gap between FZ 5 and FZ 11.

5.4. Carbonate carbon isotope composition

A total of 23 samples passed the screening tests (Figure 4). The mean $\delta^{13}C_{carb}$ value is 2.2‰ with standard deviation of 0.55. The lower part of the succession (FZ 1 – FZ 3 zonal interval) shows highly variable values of $\delta^{13}C_{carb}$ fluctuating from 1.8‰ to 2.7‰. The highest values occur in the middle part of the succession. In peaks they reach 3.5‰ in the lowermost FZ 4 and 3.1‰ at the base of FZ 5. The lowermost values (c.a. 1.3‰) characterize the uppermost part of the succession (FZ 11 – FZ 13a zonal interval). In general, the carbonate carbon isotope record shows intermediate values in the FZ 1 – FZ3 zonal interval, the plateau with quite high values in the FZ 4 – FZ 5 zonal interval, and low values in the FZ 11 – FZ 13a zonal interval.

6. Discussion

6.1. Relative sea-level changes at the Bolshaya Nadota section

The section of the Bolshaya Nadota river lacks part of the Frasnian sediments in the interval of FZ 6 – FZ 10 due to tectonic reasons.

The transition from MF-2 (Member 1) to MF-3 (Member 2) probably corresponds to regression. The erosional surface at the base of Member 2 suggests reworking of part of the FZ 1 sediments. The subsequent transition from MF-3 (Member 3a) to MF-1 (Member 3b) probably corresponds to a transgression correlated with the global Genundewa Event (House and Kirchgasser, 1993) and corresponds to the base of the

IIb-2 cycle of North America (Johnson et al., 1985; Day et al., 1996; Day, 1998). The abrupt transition from MF-1 (Member 3b) to MF-3 (Member 4) probably corresponds to regression with an erosional surface at the base of Member 4. This erosion may have destroyed the sediments of the upper part of FZ 3 and the lower part of FZ 4. The change from the MF-3 (Member 4) to MF-1 (Member 5) is considered as probable sign of the transgression. Given the possible partial absence of sediments from FZ 3 and FZ 4, it can be assumed that this transgression is an echo of the Timan Event. The abrupt transition from MF-1 (Member 5) to MF-4 (Member 6a) probably corresponds to a regression with an erosion surface at the base of Member 6a. This erosion may have destroyed the sediments of part of FZ 4. The transition from MF-4 (Member 6a) to MF-3 (Member 6b) represents a gradual transgression. This transgression may correspond to *punctata*/Middlesex Event. The erosional surface at the base of overlying Member 6c marks regression. The corresponding gap probably comprises the some part of FZ 5.

The change from the MF-2 (Member 7 and lower part of Member 8) to MF-1 (Member 8) is considered as probable sign of the late Frasnian gradual transgression correlated with Lower Kellwasser Event.

The sequence of microfacies in the studied section allowed us to reconstruct sea level changes (Figures 4 and 5). The conodont zones provided a reliable framework for regional and global correlation of sea level changes and events (Becker et al., 2016). A significant sea level rise is recorded around the FZ 2 – FZ 3 boundary, suggesting the occurrence of the Genundewa Event.

6.2. Genundewa Event

The Frasnian Matyashor Formation in Olysya Mountain area is mainly contains massive microbial-algal limestones (framestones) and bioclastic limestones (wackestones, packstones, and floatstones) with a massive or lenticular-layered structure formed in an isolated carbonate platform of the shelf edge environments. A significant part of the Frasnian is characterized by calm-water conditions of microfacies MF-1 (wackestone) and MF-3 (floatstone) and moderately active water conditions of microfacies MF-2 (packstone) and MF-4 (framestone).

The conodont assemblages indicate that the studied sequence comprises an interval from Frasnian Zone 1 to FZ 13a with a gap between FZ 5 and FZ 11. A significant sea level rise is recorded around the FZ 2 – FZ 3 boundary, suggesting the occurrence of the Genundewa Event. The Frasnian conodont Zone 2 is indicated by the presence of the index species *Ancyrodella rotundiloba* (Bryant), and the FZ 3 by the typical forms of *Ancyrodella recta* Kralick. The presence of a fauna of conodonts, brachiopods and ostracods in the event interval suggests normally marine conditions without signs of anoxia. Although in many regions the Genundewa Event is accompanied by the onset of oxygen-deficient facies (House and Kirchgasser, 1993; House, 2002).

The Genundewa Event can be recognized by a remarkable facies shift from floatstone with a massive structure to a succession of microlaminated wackestone in the Member 3b. This transition from floatstone of MF-3 to wackestone of MF-1 corresponds to the transgression. The Member 3b is represented by deposits about 2 meters thick yielding a diverse conodont fauna. In the FZ 2 – FZ 3 boundary interval, corresponding to the Genundewa Event, there is a dominance of *Polygnathus*, *Ancyrodella*, and *Mesotaxis* whereas in the underlying shallow-water deposits the genus *Polygnathus* clearly predominated. *Polygnathus* is the most abundant genus in FZ 2 below the event interval.

Specimens of other genera *Ancyrodella*, *Icriodus*, and *Youngquistognathus* are rare. From the onset of the deep-water MF-1 in the event interval there is a predominance of *Polygnathus* and *Ancyrodella*. *Mesotaxis* also constitutes important component of the conodont assemblage, but its abundance is not high. Specimens of other genera *Icriodus* and *Zieglerina* are rare in the event interval. The small number of conodonts in the studied section does not allow us to distinguish biofacies, but we can assume that the polygnathid-ancyrodellid biolfacies developed predominantly during the Genundewa event interval. This indirectly indicates the deepening of the basin at this time, which is supported by lithological data.

The Genundewa Event is often poorly recognised in shallow water facies in other regions due to the absence or low abundance of the Ancyrodella conodont fauna and numerous gaps. However, by studying sedimentation cycles and examining conodont and other fauna, it is sometimes possible to identify this transgression in the shallow water reef facies. For example, the transgressive event close to the Genundewa Event was characterized by Racki (1993) in the shallow-water carbonate platform and reef facies Holy Cross Mts, Poland. In these facies the event is manifested by appearance of calcarenites and calcilutites in the succession of coral and stromatoporoid limestones and corresponds to the beginning of Poland IC cycle (Racki, 1988, 1993; Racki and Bultynck, 1993).

The manifestation of the Genundewa Event in shallow-marine environments in the Southern Timan (Russia) was described by us earlier (Sobolev et al., 2023). This event is marked by bioclastic and micritic limestones with sparse clay interbeds overlying terrigenous quartz siltstones and silty limestones. In the event interval the input of terrigenous quartz material ceases completely. The fauna in these sediments is

represented by *Styliolina*, brachiopods, gastropods, crinoids, ostracods, and conodonts of FZ 2 – FZ 3. The event's onset corresponds to the start of a significant sedimentation cycle and the base of the Sargaevian regional substage of the Urals and Russian Platform (Rodionova et al., 1995; Tikhomirov, 1995).

The preserved deposits corresponding to the Genundewa Event represent MF-1, which manifests the short-term deepening episode on the extremely shallow water background. This deepening led to the disappearance of algal and microbial assemblages, the appearance of brachiopods, crinoids and changes in conodont biofacies. Traces of other Frasnian eustatic events, such as Frasne, Timan, Middlesex, Lower Kellwasser, were poorly preserved in the Bolshaya Nadota river section, probably due to the numerous episodes of erosion and tectonic reasons.

6.3. Early-Middle Frasnian carbon isotope perturbation

In general, a positive carbon isotope anomaly occurs in the studied succession (Figure 4). The anomaly covers a stratigraphic interval from the FZ 4 (= *Pa. transitans* Zone) to the FZ 11 – FZ 13a zonal interval (= *Pa. jamieae* – *Pa. rhenana* zonal interval). The age and structure of the carbon isotope anomaly agree with those of the Early-Middle Frasnian carbon isotope perturbation reported by Pisarzowska et al. (2006, 2020).

Following the data of Pisarzowska et al. (2006), it is possible to distinguish four events composing the anomaly. The positive excursion of 3.5‰ in FZ 4 probably corresponds to the first event. The subsequent negative shift corresponds to the second event. The broad positive excursion of 3‰ in FZ 5 corresponds to the main (third) event. A similar magnitude of this positive excursion has been reported from the facies of the intrashelf depression in the Pechora Basin (Kotik et al., 2021). The subsequent gradual decrease

of $\delta^{13}C_{carb}$ values in the FZ 11 – FZ 13a zonal interval can be correlated with the fourth (last) event of the Early-Middle Frasnian carbon isotope perturbation. The early entry of this isotopic event in the studied section in the lower part of FZ 4 may be caused by the incompleteness of the sedimentary record and the presence of a gap at the base of FZ 4. There is no evidence for the significant carbon isotope changes in the Genundewa Event interval preceding the Early-Middle Frasnian carbon isotope perturbation (Figure 4). The magnitude of $\delta^{13}C_{carb}$ shifts in the Early-Middle Frasnian interval in the studied section (~3‰) is similar to those reported from hemipelagic facies around the world (Pisarzowska et al., 2020). This similarity may reflect increased water exchange between the ocean and the isolated carbonate platform during the Early-Middle Frasnian.

Conclusion

Evidence of the Frasnian Genundewa Event was detected in the facies of the isolated carbonate platform in Sub-Polar Urals. The event interval is biostratigraphically constrained. It corresponds to the boundary of FZ 2 and FZ 3 conodont zones. The FZ 2 is indicated by the presence of the index species *Ancyrodella rotundiloba* (Bryant), and the FZ 3 is indicated by the typical forms of *Ancyrodella recta* Kralick. The event is marked by appearance of the deep-water micritic microlaminated carbonates (MF-1) in the shallow-water carbonate succession. *Polygnathus, Ancyrodella,* and *Mesotaxis* predominant here. *Polygnathus* is the most abundant genus in FZ 2 below the event interval. The Early-Middle Frasnian carbon isotope perturbation is detected above the Genundewa Event. No specific features of the event interval in the C-isotope record are observed. The mean $\delta^{13}C_{carb}$ value is about 2‰ in the event interval. The start of the

Genundewa Event marks the beginning of Euro-American IIb2 cycle and is correlated with the base of the Sargaevian regional substage of the Urals and Russian Platform and the base of Poland IC cycle. This confirms the global character of this event.

Acknowledgment

This work was supported by the project № 122040600008-5 of the N.P. Yushkin Institute of Geology Komi SC UrB RAS (Syktyvkar, Russia) and partially by RFBR grant № 20-05-00445. Isotope analysis was performed at the CKP "Geonauka" of the Institute of Geology Komi SC UrB RAS. We thank I.V. Smoleva for isotope data. The authors would like to thank V.A. Radaev (Institute of Geology Komi SC UrB RAS) for assistance with the SEM work and L.I. Kononova (Moscow State University, Moscow, Russia) for consultations on conodonts. We thank R.S. Karmanov, S.Yu. Kamzalakova, V.A. Konovalova for joint field work on the Bolshaya Nadota river.

References

Aboussalam ZS (2003). Das ‘‘Taghanic-Event’’ im höheren Mittel-Devon von West-Europa und Marokko. Münstersche Forschungen zur Geologie und Paläontologie 97: 1-332.

Aboussalam ZS, Becker RT (2007). New upper Givetian to basal Frasnian conodont fauna from the Tafilalt (Anti-Atlas, southern Morocco). Geological Quarterly 51: 345-374.

Baird GC, Kirchgasser WT, Over DJ, Brett CE (2006). An early late Devonian bone-bed-pelagic limestone succession: The North Evans–Genundewa Limestone story. In

Jacobi R (Ed.), New York State Geological Association Field Trips (Guidebook): 354-395.

Becker RT, House MR (1997). Sea level changes in the Upper Devonian of the Canning Basin. Courier Forschungsinstitut Senckenberg 199: 129-146.

Becker RT, Königshof P, Brett CE (2016). Devonian climate, sea level and evolutionary events: an introduction. Geological Society, London Special Publications 423: 1-10. http://doi.org/10.1144/SP423.15

Becker RT, Marshall JEA, Da Silca A-C, Agterberg FP, Gradstein F et al. (2020). The Devonian Period. In F Gradstein, J G Ogg, M D Schmitz, GM Ogg (Eds.). Geological Time Scale 2020, 2. Amsterdam: 733–810. http://doi.org/10.1016/B978-0-12-824360-2.00022-X

Day J (1998). Distribution of latest Givetian-Frasnian Atrypida (Brachiopoda) in central and western North America. Acta Palaeontologica Polonica 43(2): 205-240.

Day J, Uyeno T, Norris W, Witzke BJ, Bunker BJ (1996). Middle-Upper Devonian relative sea-level histories of central and western North American interior basins. In BJ Witzke, GA Ludvigson, J Day (Eds.). Paleozoic Sequence Stratigraphy: Views from the North America Craton: Boulder, Colorado. Geological Society of America, Special Paper 30: 259-275.

Dunham RJ (1962). Classification of carbonate rocks according to depositional texture. In: Ham WE, editor. Classification of Carbonate Rocks. A Symposium. AAPG Memoir 1. Tulsa, OK, USA: AAPG, pp. 108-171.

Eliseev AI (1978). Formations of limit zones north-east European platform. Leningrad: 204 pp. (In Russian).

Gruzdev DA (2017). Late Devonian-Early Carboniferous isolated carbonate platform in the Subpolar Urals (Bol. Nadota river). Vestnik IG Komi SC UB RAS 4 (268). 16-23 (In Russian). https://doi.org/10.19110/2221-1381-2017-4-16-23

Gruzdev DA (2021). Late Devonian-Early Carboniferous isolated carbonate platforms of the North of the Urals and Pay-Khoy. Vestnik of Geosciences 10(322): 3-15 (In Russian). https://doi.org/10.19110/geov.2021.10.1

Gruzdev DA, Soboleva MA, Sobolev DB, Zhuravlev AV (2016). The Frasnian deposits in the Bol'shaya Nadota River region (Sub-Polar Urals) – stratigraphy and depositional enviroment. Lithosphere (Russia) 6: 97-116 (in Russian).

Gruzdev DA, Zhuravlev AV (2003). Conodonts of Matyashor strata (Devonian Bolshaya Nadota district). Vestnik IG Komi SC UB RAS (1): 14-16 (In Russian).

Hammer Ø., Harper DAT, Ryan PD (2001). PAST: Paleontological statistics software package for education and data analysis. Palaeontologia Electronica 4(1): 9 pp.

Hinde GJ (1879). On conodonts from the Chazy and Cincinnati Group of the Cambro-Silurian, and from the Hamilton and Genesee shale divisions of the Devonian, in Canada and the United States. Quarterly Journal of the Geological Society of London 35: 351-369.

House MR (2002). Strength, timing, setting and cause of mid-Palaeozoic extinctions. Palaeogeography, Palaeoclimatology, Palaeoecology 181: 5-25. https://doi.org/10.1016/S0031-0182(01)00471-0

House MR, Kirchgasser WT (1993). Devonian goniatite biostratigraphy and timing of facies movements in the Frasnian of eastern North America. Geological Society, London Special Publications 70: 267-292. https://doi.org/10.1144/GSL.SP.1993.070.01.19

House MR, Menner VV, Becker RT, Klapper G, Ovnatanova NS et al. (2000). Reef episodes, anoxia and sea-level changes in the Frasnian of the southern Timan (NE Russian Platform). Geological Society, London Special Publications 178: 147-176.

Johnson JG, Klapper G, Sandberg CA (1985). Devonian eustatic fluctuations in Euramerica. Geological Society of America Bulletin 96: 567-587. https://doi.org/10.1130/0016-7606(1985)96<567:DEFIE>2.0.CO;2

Kimmel RE (1973). Implications of Photogeologic Linears in the South Long Lake Area, Alpena and Presque Isle Counties, Michigan. Master's Theses. 615.

Klapper G (1989). The Montagne Noire Frasnian (Upper Devonian) conodont succession. In: McMillan NJ, Embry AF, Glass DJ (eds.) Devonian of the World. Calgary, Canadian Society of Petroleum Geologists Memoir 14 (III): 449-468 [Imprint 1988].

Klapper G, Kirchgasser WT (2016). Frasnian Late Devonian conodont biostratigraphy in New York: graphic correlation and taxonomy. Journal of Paleontology 90 (3): 525-554. https://doi.org/10.1017/jpa.2015.70

Klapper G, Uyeno TT, Armstrong DK, Telford PG (2004). Conodonts of the Williams Island and Long Rapids formations (Upper Devonian, Frasnian–Famennian) of the Onakawana B Drillhole, Moose River Basin, northern Ontario, with a revision of Lower

Famennian species. Journal of Paleontology 78(2): 371-387. https://doi.org/10.1666/0022-3360(2004)078<0371:COTWIA>2.0.CO;2

Kotik IS, Zhuravlev AV, Maydl TV, Bushnev DA, Smoleva IV (2021). Early-Middle Frasnian (Late Devonian) carbon isotope Event in the Timan-Pechora Basin (Chernyshev Swell, Pymvashor River section, North Cis-Urals, Russia). Geologica Acta 19.3: 1-17. https://doi.org/10.1344/GeologicaActa2021.19.3

Kralick JA (1994). The conodont genus *Ancyrodella* in the Middle Genesee Formation (Lower Upper Devonian, Frasnian), western New York. Journal of Paleontology 68(6): 1384-1395. https://doi.org/10.1017/S0022336000034351

Müller KJ, Clark DL (1967). Early Late Devonian conodonts from the Squaw Bay Limestone in Michigan. Journal of Paleontology 41 (4): 902-919.

Pisarzowska A, Becker RT, Aboussalam ZS, Szczerbac M, Sobieńd K et al. (2020). Middlesex/*punctata* Event in the Rhenish Basin (Padberg section, Sauerland, Germany) – Geochemical clues to the early-middle Frasnian perturbation of global carbon cycle. Global and Planetary Change 191. https://doi.org/10.1016/j.gloplacha.2020.103211

Pisarzowska A, Sobstel M, Racki G (2006). Conodont−based event stratigraphy of the Early–Middle Frasnian transition on the South Polish carbonate shelf. Acta Palaeontologica Polonica 51 (4): 609-646.

Puchkov VN (1979). Bathyal complexes of geosynclinal regions passive margins. Moscow: 260 pp. (In Russian).

Raaben ME (1959). Stratigraphy of the ancient formations of the Polar Urals. Moscow: 131 pp. (In Russian).

Racki G (1988). Middle to Upper Devonian boundary beds of the Cross Mts, Central Poland: Introduction to ecostratigraphy. Canadian Society of Petroleum Geologists 14 (3): 119- 131.

Racki G (1993). Evolution of the bank to reef complex in the Devonian of the Holy Cross Mountains. Acta Palaeontologica Polonica 37 (2-4): 87-182.

Racki G (2005). Toward understanding Late Devonian global events: few answers, many questions. Understanding Late Devonian and Permian-Triassic Biotic and Climatic Events: towards an integrated approach. Developments in Palaeontology and Stratigraphy. Elsevier (20): 5-36. https://doi.org/10.1016/S0920-5446(05)80002-0

Racki G, Bultynck P (1993). Conodont biostratigraphy of the Middle to Upper Devonian boundary Beds in the Kielce area of the Holy Cross Mts. Acta Palaeontologica Polonica 43 (1-2): 1-25.

Rodionova GD, Umanova VT, Kononova LI, Ovnatanova NS, Rzhonsnitskaya MA et al. (1995). Devonian of the Voronezh anteclise and Moscow Syneclise. Moscow: 265 pp. (In Russian).

Sandberg CA, Ziegler W, Dreesen R, Butler JL (1988). Late Frasnian mass extinction: conodont event stratigraphy, global changes, and possible causes. Contribution 1: Courier Forschungsinstitut Senckenberg 102: 263-307.

Saupe F, Becker RT (2022). Refined conodont stratigraphy at Martenberg (Rhenish Massif, Germany) as base for a formal middle/upper Frasnian substage boundary. Palaeobiodiversity and Palaeoenvironments 102: 711-761. https://doi.org/10.1007/s12549-022-00537-z

Skompski S, Paszkowski M, Krobicki M, Kokovin K, Korn D et al. (2001). Depositional setting of the Devonian/Carboniferous biohermal Bol'shaya Nadota Carbonate Complex, Subpolar Urals. Acta Geologica Polonica 51 (3): 217-235.

Sobolev DB, Soboleva MA, Evdokimova IO (2023). Ostracod zonation of the Givetian-Frasnian boundary interval in the Timan-North Urals Region. Lithosphere (Russia) 23(3): 348-366. (in Russian). https://doi.org/10.24930/1681-9004-2023-23-3-348-366

Sobolev DB, Zhuravlev AV, Karmanov RS, Gruzdev DA (2000). New data on the geological structure of the Bolshaya Nadota reef (Sub-Polar Urals). Vestnik of IG Komi SC UB RAS 8 (68): 6-7 (in Russian).

Soboleva MA, Sobolev DB, Matveeva NA (2018a). Frasnian section of the Kozhim River (the western slope of SubPolar Urals) results of biostratigraphic, bio- and lithofacies, isotopic and geochemical studies. Petroleum Geology – Theoretical and Applied Studies: 13(1). (in Russian). https://doi.org/10.17353/2070-5379/2_2018

Soboleva MA, Sobolev DB, Matveeva NA (2018b). Lithology and biostratigraphy of the Frasnian and border section on the Kosyu River (Subpolar Urals). Petroleum Geology - Theoretical and Applied Studies: 13(4). (in Russian). https://doi.org/10.17353/2070-5379/43_2018

Shishkin MA (1989). Tectonics of the South Lemva zone (Polar Urals). Geotektonika (3): 86-95 (in Russian).

Shishkin MA (1999). Stratigraphic scheme of partition of Paleozoic rocks on the western slope of the Polar Urals and Chernyshev Ridge applied to the problems of drawing up a new generation of geological maps of scale 1:200 000. The Geology and

mineral resources of the European North-East of Russia. The new findings and new perspectives 2: 247-249 (In Russian).

Shishkin MA (2003). Geology of the junction zone Elets and Lemva facies in the western slope of the Polar Urals. Cand. geol. and min. sci. absr. diss.: 20 pp. (In Russian).

Tikhomirov SV (1995). Stages of sedimentation of the Devonian of the Russian Platform and general questions of stratisphere development and construction. Moscow: 445 pp. (In Russian).

Timonin NI (1998). Pechora Plate: a history of geological evolution in the Phanerozoic (in Russian). Ural Branch of the Russian Academy of Sciences: 240 pp. (In Russian).

Voinovsky-Kriger KG (1945). Two Paleozoic complex on the western slope of the Polar Urals. Soviet geology (6): 27-44 (In Russian).

Walliser OH (1996). Global events in the Devonian and Carboniferous. Global events and event stratigraphy in the Phanerozoic. Springer: 225-250.

Yudin VV (1994). Orogenesis of the North Urals and Pay-Khoy (in Russian). Ekaterinburg, Nauka: 284 pp. (In Russian).

Zhuravlev AV (2002). Upper Givetian and Lower Frasnian conodonts from the "Olysia" Reef (Subpolar Urals). Geology of the Devonian System: 161-163.

Zhuravlev AV, Plotitsyn AN, Gruzdev DA (2020). Carbon isotope stratigraphy of the Tournaisian (Lower Mississippian) successions of NE Europe. Stratigraphy & timescales 5. 467-527. https://doi.org/10.1016/bs.sats.2020.08.007

Ziegler W, Sandberg CA (1990). The Late Devonian Standard Conodont Zonation. Courier Forschungsinstitut Senckenberg 121: 1-114.

Ziegler W, Sandberg CA (2000). Utility of Palmatolepids and Icriodontids in recognising Upper Devonian Series, Stage, and possible Substage boundaries. Courier Forschungsinstitut Senckenberg 225: 335-347.

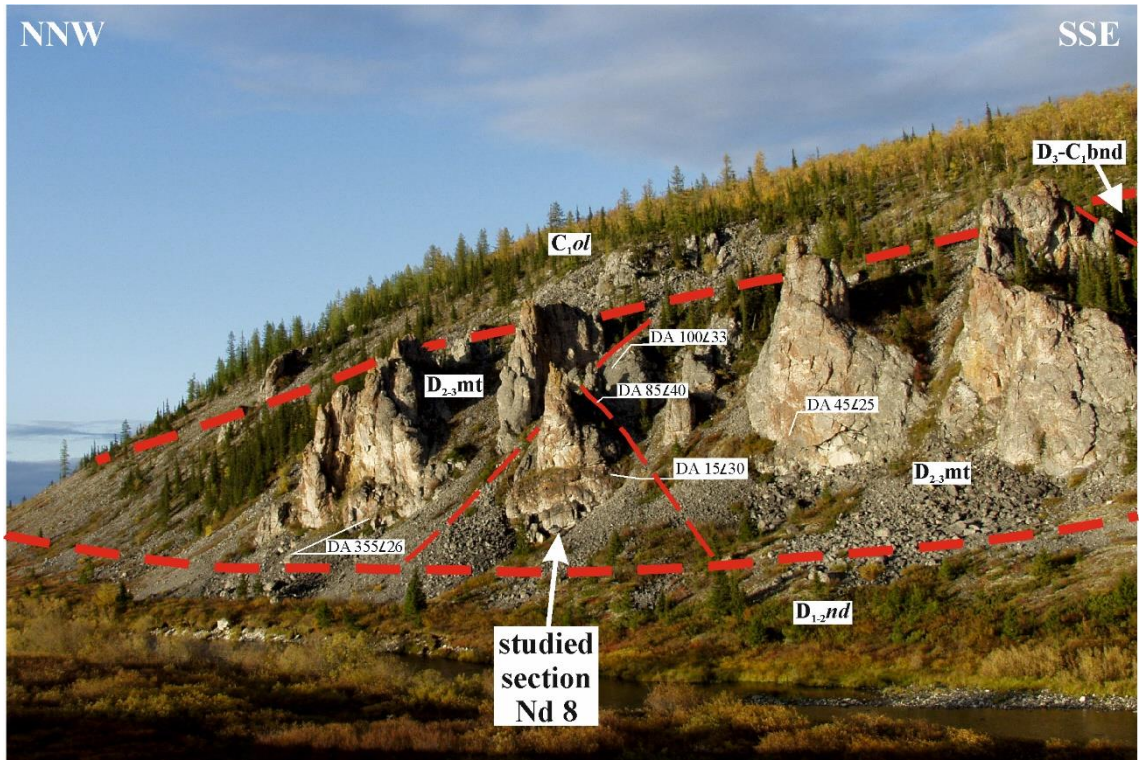

Figure 1. Panoramic view of the Devonian-Carboniferous succession, from the Nadotamylk Formation ($D_{1\text{-}2}$nd), through the Matyashor ($D_{2\text{-}3}$mt) and the Bolshaya Nadota formations (D_3-C_1bol), to the Olysya Reef Massif (C_1ol) on the southern slope of Olysya Mountain. The boundaries between formations are shown in red.

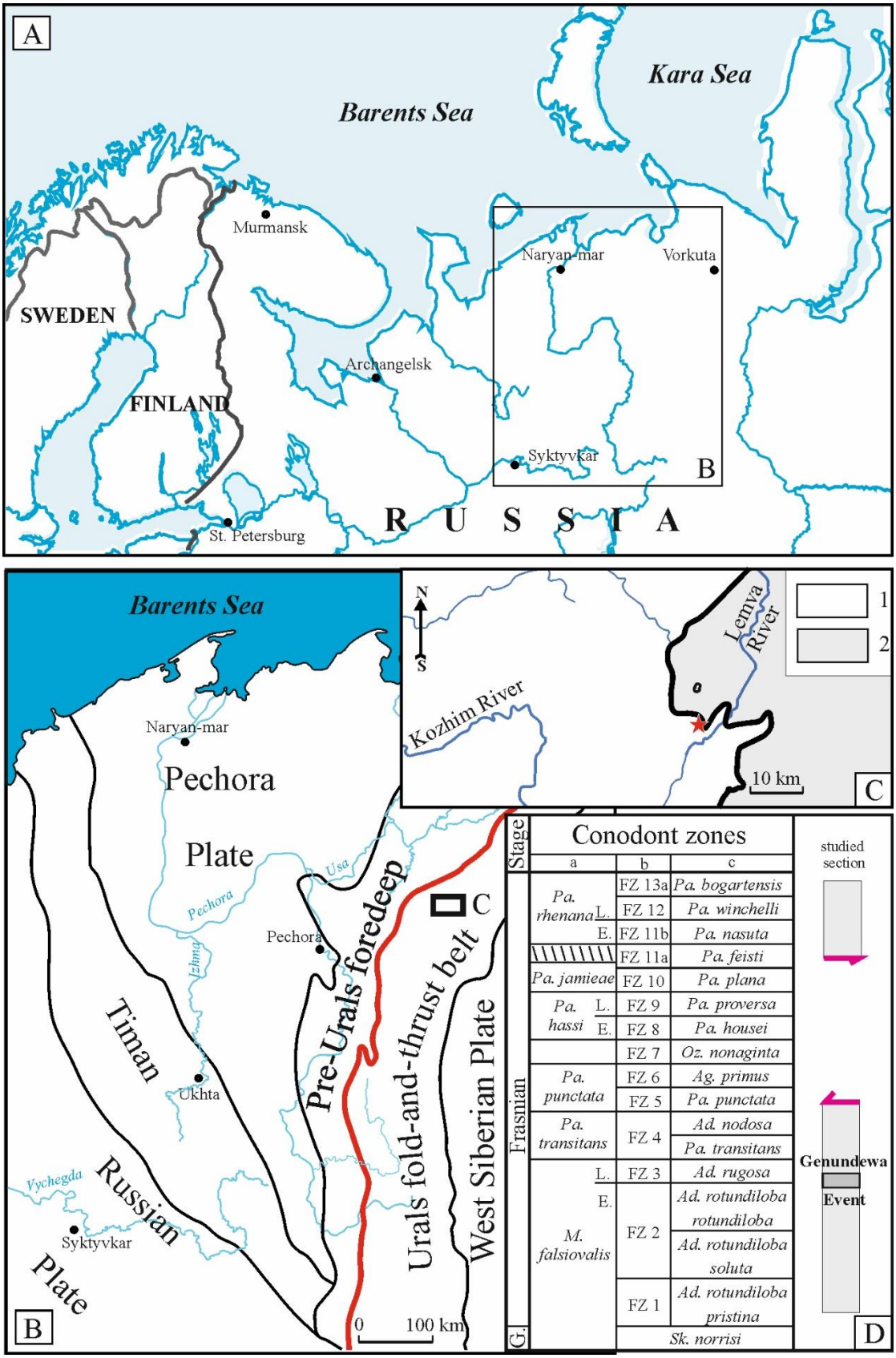
A
Barents Sea
Kara Sea
Murmansk
Naryan-mar
Vorkuta
SWEDEN
Archangelsk
FINLAND
Syktyvkar
B
RUSSIA
St. Petersburg
Barents Sea
N
S
Lemva River
1
2
Kozhim River
10 km
C
Naryan-mar
Pechora
Plate
Usa
Pechora
Pechora
Izhma
Timan
Ukhta
Pre-Urals foredeep
C
Urals fold-and-thrust belt
West Siberian Plate
Vychegda
Russian
Syktyvkar
Plate
B
0
100 km
Stage
Conodont zones
a
b
c
Frasnian
Pa. rhenana
L.
E.
FZ 13a
FZ 12
FZ 11b
FZ 11a
Pa. bogartensis
Pa. winchelli
Pa. nasuta
Pa. feisti
Pa. jamieae
FZ 10
Pa. plana
Pa. hassi
L.
E.
FZ 9
FZ 8
Pa. proversa
Pa. housei
FZ 7
Oz. nonaginta
Pa. punctata
FZ 6
FZ 5
Ag. primus
Pa. punctata
Pa. transitans
FZ 4
Ad. nodosa
Pa. transitans
L.
E.
M. falsiovalis
FZ 3
FZ 2
FZ 1
Ad. rugosa
Ad. rotundiloba rotundiloba
Ad. rotundiloba soluta
Ad. rotundiloba pristina
Sk. norrisi
G.
studied section
Genundewa Event
D

1

Figure 2. A) Location of the Timan-Pechora Province (B) in Russia. B) Location of the studied area on the tectonic scheme of the Timan-Pechora Province, Russia. Black rectangle marks location of map shown in C; red line correspond to Main West Uralian Thrust. C) Tectonic map fragment (Shishkin, 2003; with modification). Legend: West Ural Structural Zone. 1) autokhtone (shelf formations), 2) allokhtone (bathyal formations). D) Correlation of the Frasnian conodont zones. a. Standard conodont zones according to Ziegler and Sandberg (1990, 2000); b. Frasnian conodont zones (FZ) according to Klapper (1989) and Klapper and Kirchgasser (2016); c. Conodont zones according to Becker et al. (2020: in Devonian Time Scale) and Saupe and Becker (2022). *Ad: Ancyrodella, Ag: Ancyrognathus, M: Mesotaxis, Oz: Ozarkodina, Pa: Palmatolepis, Sk: Skeletognathus.* L: Lower, U: Upper, G: Givetian.

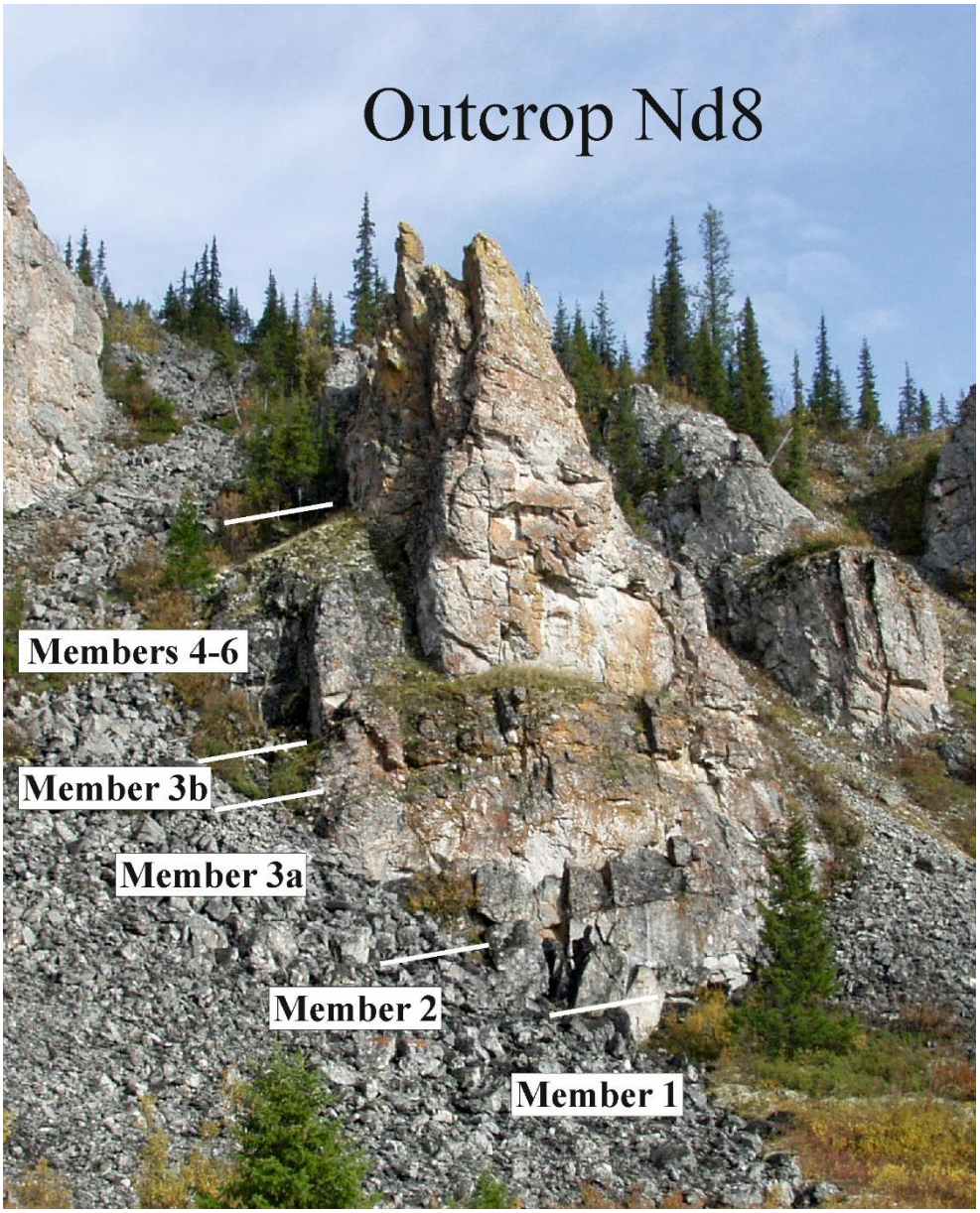

Figure 3. General view of the Frasnian Matyashor Formation, indicating the members 1-6. It is marked in Figure 1 as Outcrop Nd8.

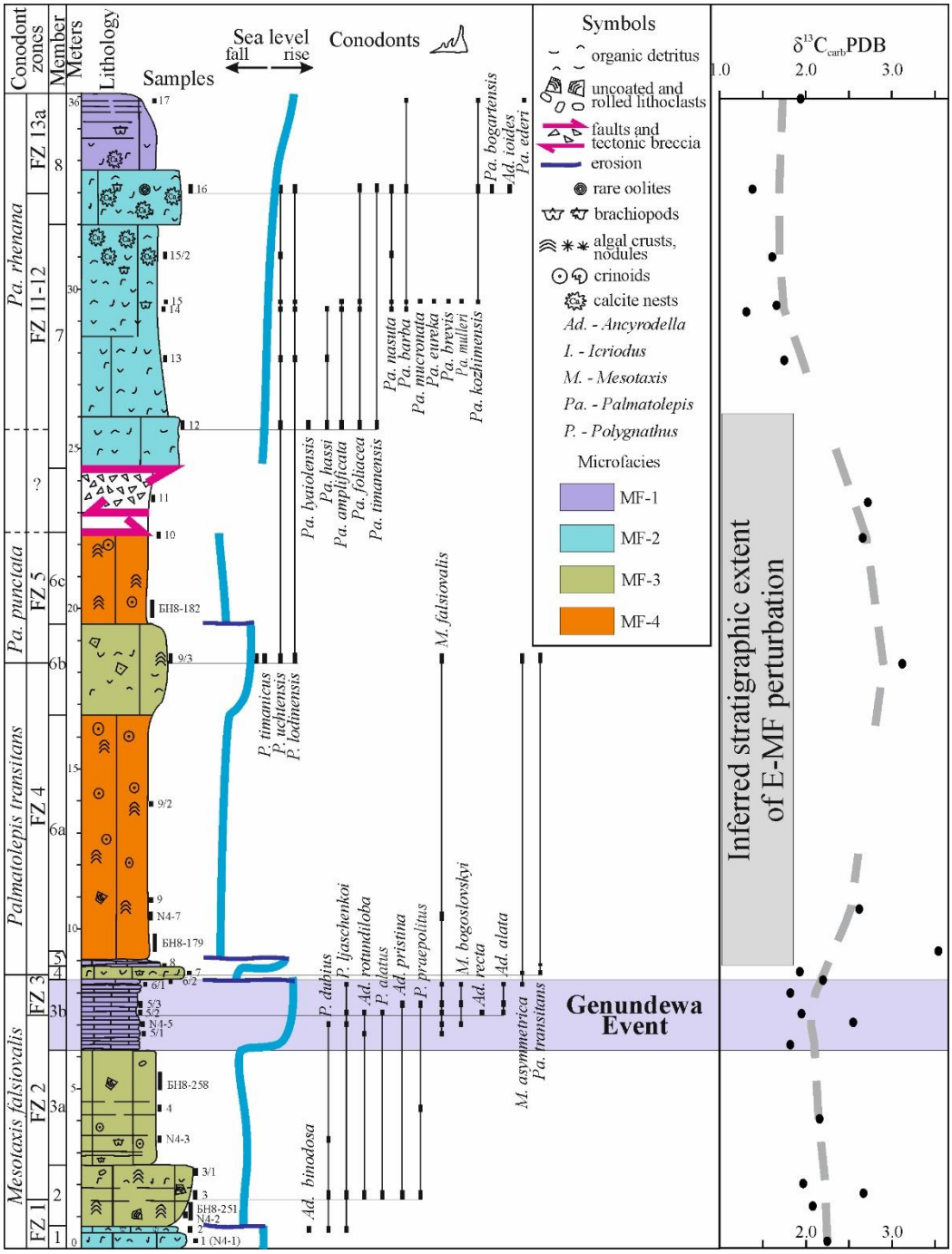

Figure 4. Stratigraphic log, conodont distribution, relative sea-level changes and Frasnian δ^{13}Ccarb profile with inferred stratigraphic extent of E-MF perturbation of studied section. Standard conodont zones according to Ziegler and Sandberg (1990) and

Frasnian conodont zones (FZ) according to Klapper (1989) and Klapper and Kirchgasser (2016). MF: Microfacies.

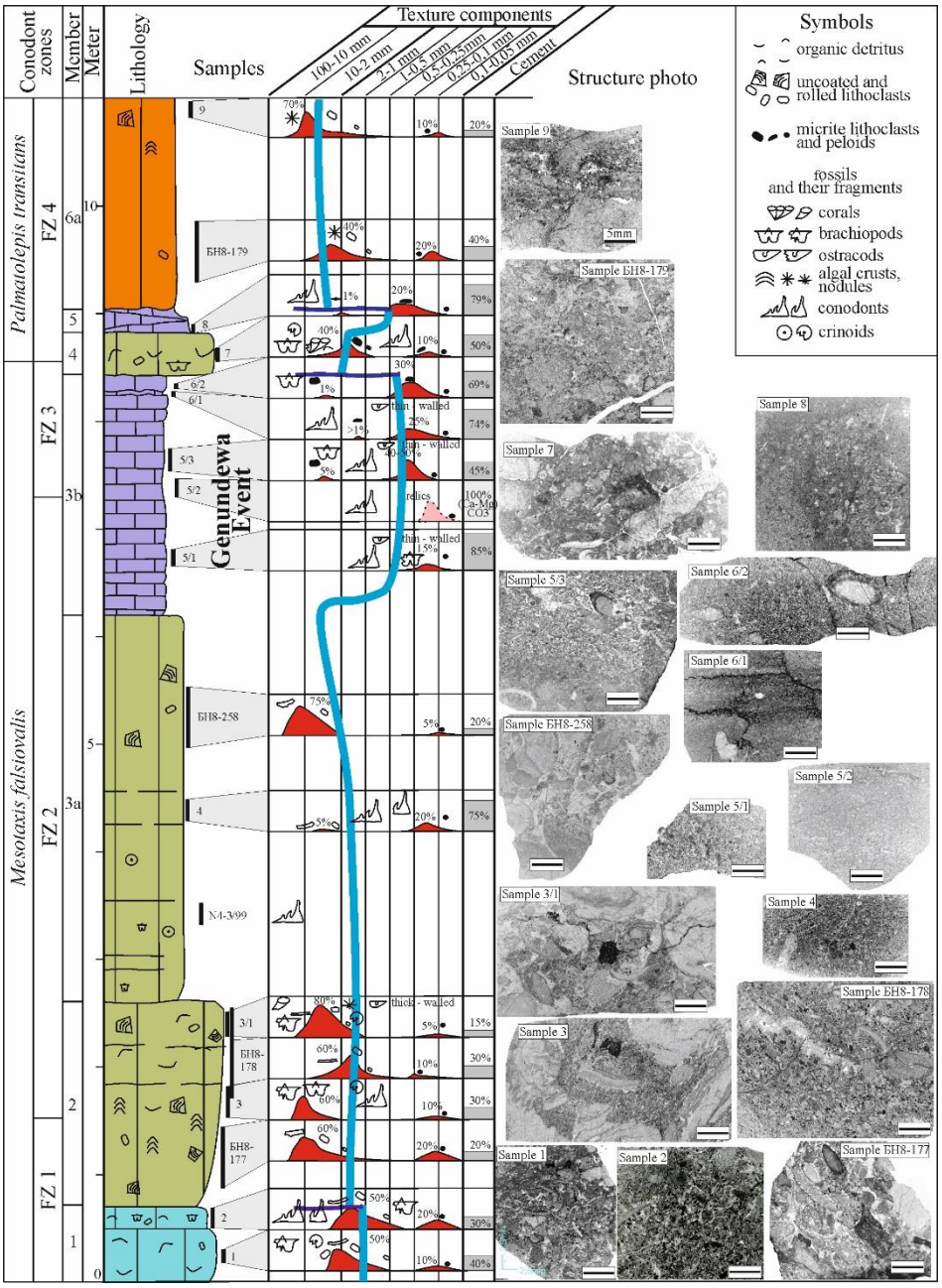

Figure 5. Bolshaya Nadota river section around the Genundewa Event: biostratigraphy, depositional textures and trends, structure photo, and relative sea-level changes.

Standard conodont zones according to Ziegler and Sandberg (1990) and Frasnian conodont zones (FZ) according to Klapper (1989) and Klapper and Kirchgasser (2016).

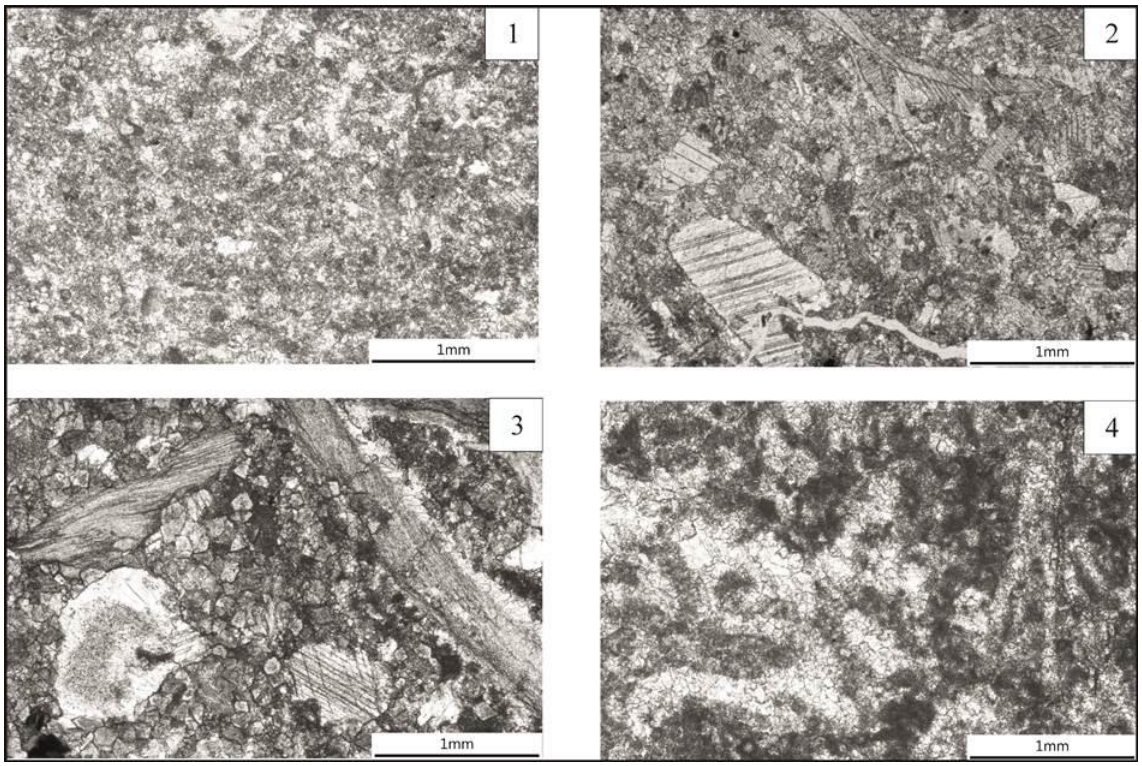

Figure 6. Thin section photomicrographs illustrating microfacies: 1 – MF-1 wackestone (Sample 6/1); 2 – MF-2 packstone (Sample 14); 3 – MF-3 floatstone (Sample 7); 4 – MF-4 framestone (Sample БН-179).

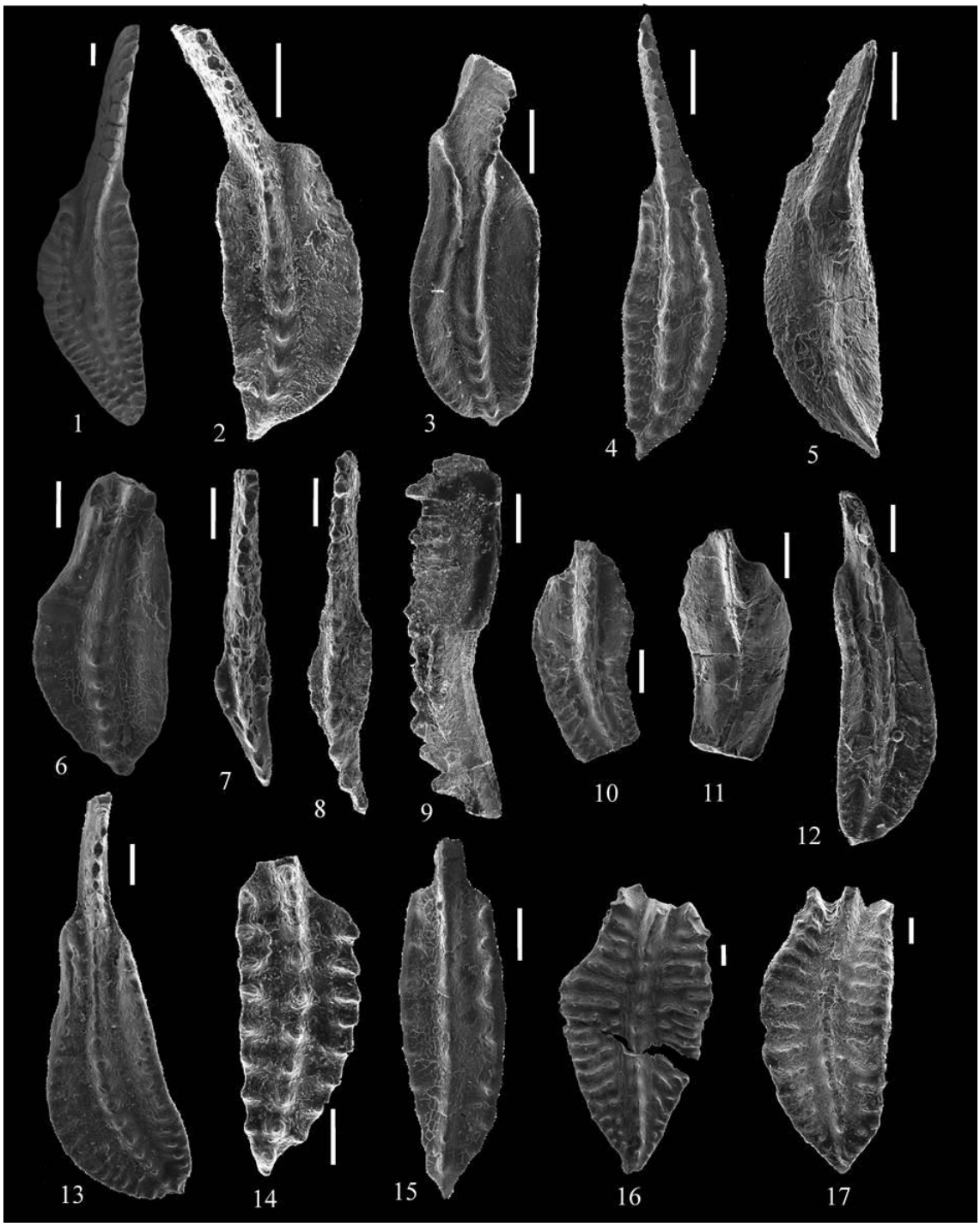

Figure 7. 1. *Polygnathus foliatus* Bryant, 1921; upper view of 492/18-10, sample 3; **2-3.** *Polygnathus alatus* Huddle, 1934, (2) upper view of 492/18-13, sample 3; (3) upper view of 492/22-21, sample 3; **4-5.** *Polygnathus pseudoxylus* Kononova, Alekseev, Braskov and Reimers, 1996; upper and lower views of 492/19-18, sample 5/3; **6.**

Polygnathus ljaschenkoi Kuzmin, 1995; upper view of 492/18-7, sample 2; **7-9.** *Youngquistognathus angustidiscus* (Youngquist, 1945); (7) upper view of 492/22-6, sample 2; (8-9) upper and lateral views of 492/23-6, sample 4; **10-12.** *Polygnathus uchtensis* Ovnatanova and Kuzmin 1991; (10-11) upper and lower views of 492/20-26, sample 9/3; (12) upper view of 492/24-14, sample 12; **13.** *Polygnathus webbi* Stauffer, 1938; upper view of 492/22-24, sample 3; **14.** *Polygnathus dengleri sagitta* Aboussalam and Becker, 2007; upper view of 492/18-18, sample 3; **15.** *Polygnathus pollocki* Druce, 1976; upper view of 492/18-14, sample 3; **16-17.** *Polygnathus pennatus* Hinde, 1879; (16) upper view of 492/22-17, sample 3; (17) upper view of 492/24-3, sample 3. Scale bar is 0.1 mm.

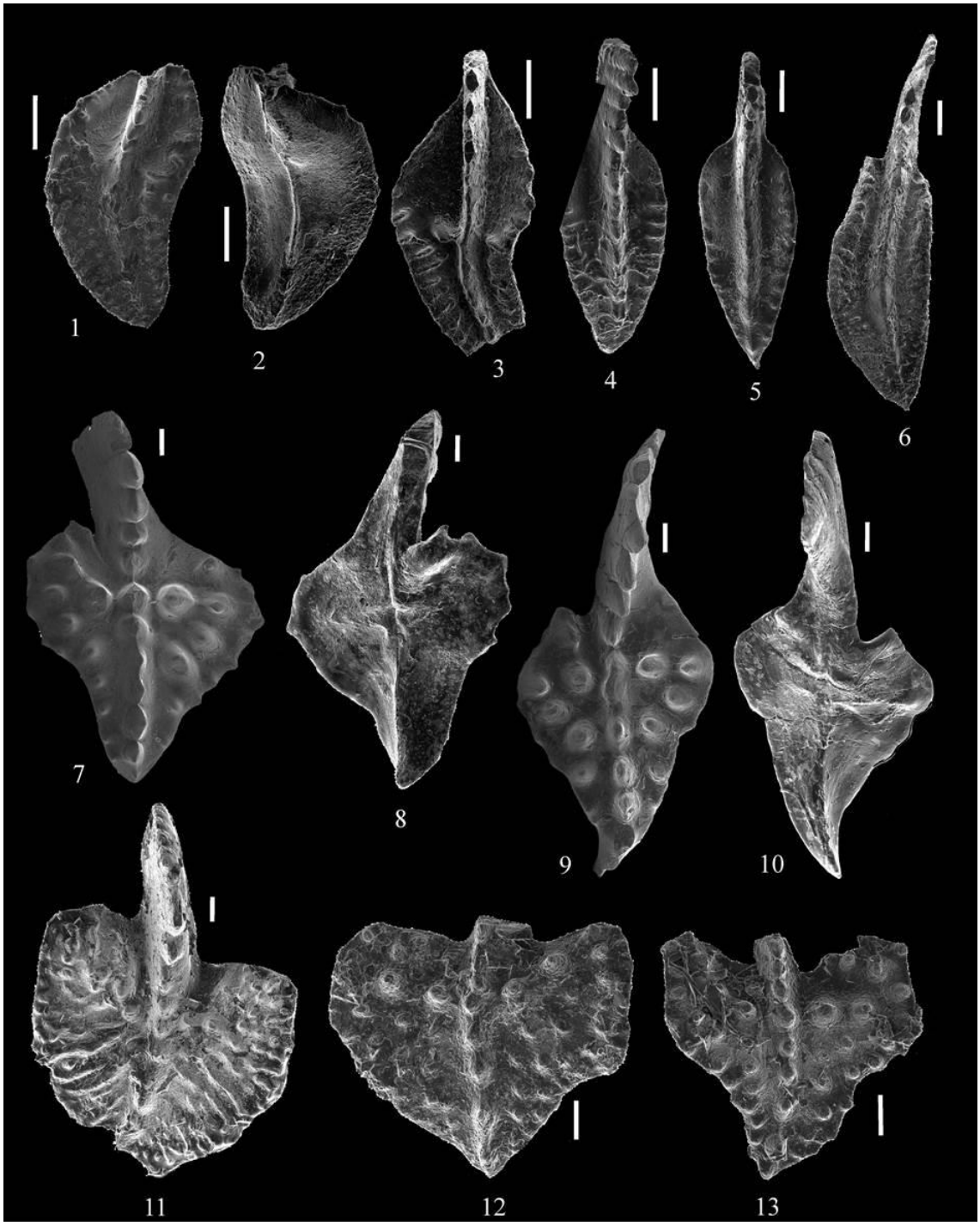

Figure 8. 1-3. *Polygnathus timanicus* Ovnatanova, 1969; (1-2) upper and lower views of 492/20-21, sample 9/3; (3) upper view of 492/23-19, sample 9/3; **4-5.** *Polygnathus lodinensis* Pölsler, 1969; (4) upper view of 492/24-18, sample 13; (5) upper view of 492/25-3, sample 14; **6.** *Polygnathus aequalis* Klapper and Lane, 1985; upper view of

492/25-1, sample 14; **7-10.** *Ancyrodella pristina* Khalymbadzha and Tchernysheva, 1970; (7-8) upper and lower views of 492/18-17, sample 3; (9-10) upper and lower views of 492/18-9, sample 3; **11.** *Ancyrodella recta* Kralick, 1994; upper view of 492/23-16, sample 5/2; **12-13.** *Ancyrodella alata* Glenister and Klapper, 1966; (12) upper view of 492/19-6, sample 5/2; (13) upper view of 492/23-15, sample 5/2. Scale bar is 0.1 mm.

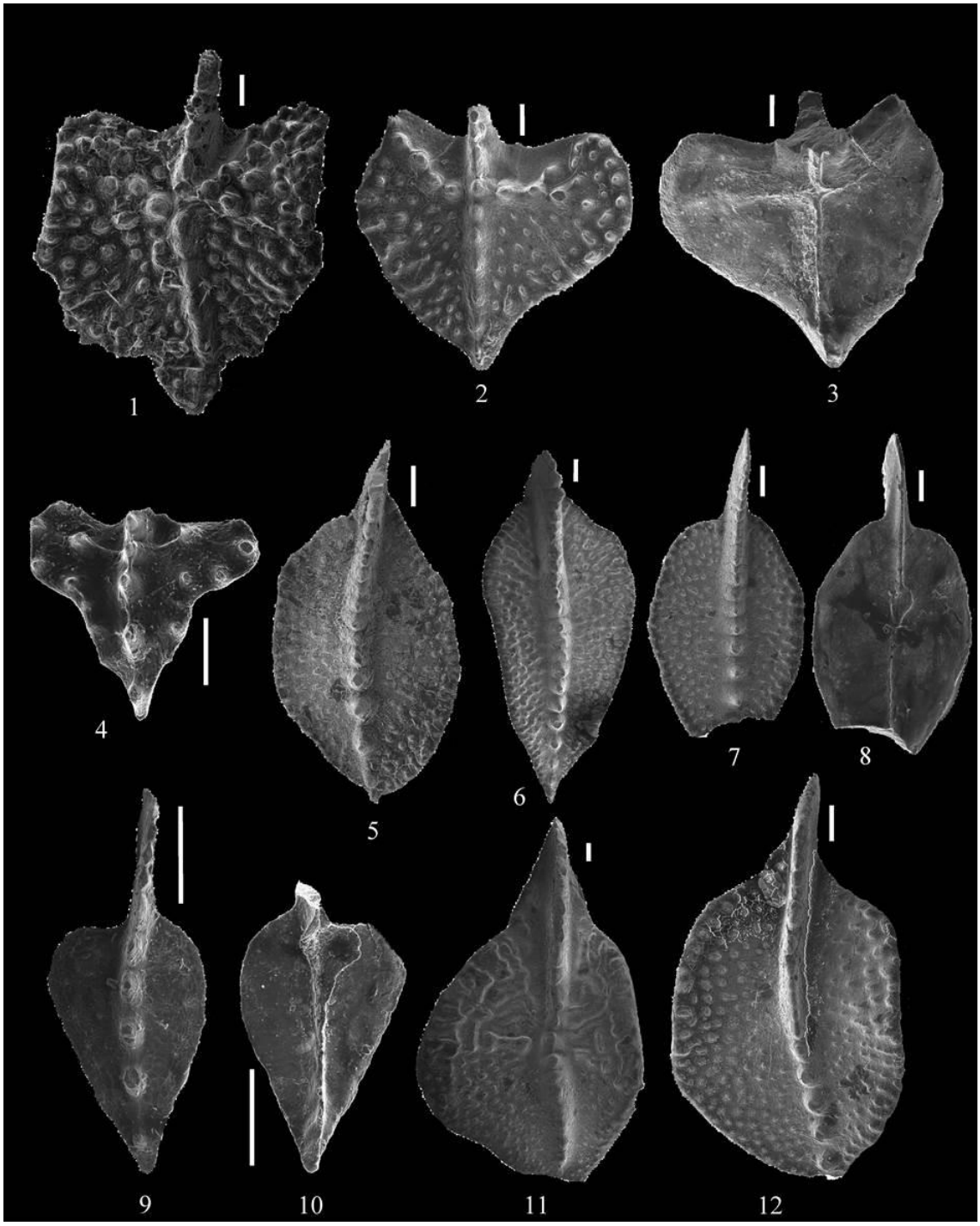

Figure 9. 1. *Ancyrodella recta* Kralick, 1994; upper view of 492/19-9, sample 5/2; **2-4.** *Ancyrodella alata* Glenister and Klapper, 1966; (2-3) upper and lower views of 492/19-11, sample 5/3; (4) upper view of 492/19-21, sample 6/1; **5.** *Zieglerina ovalis* (Ziegler and Klapper, 1964); upper view of 492/19-5, sample 5/2; **6-8.** *Mesotaxis falsiovalis*

Sandberg, Ziegler and Bultynck, 1989; (6) upper view of 492/19-15, sample 5/3; (7-8) upper and lower views of 492/19-13, sample 5/3; **9-10.** *Zieglerina nuda* Bardashev and Bardasheva, 2012; upper and lower views of 492/19-20, sample 6/1; **11.** *Palmatolepis transitans* Muller, 1956; upper view of 492/19-22, sample 7; **12.** *Mesotaxis asymmetrica* (Bischoff and Ziegler, 1956); upper view of 492/20-7, sample 9/3. Scale bar is 0.1 mm.

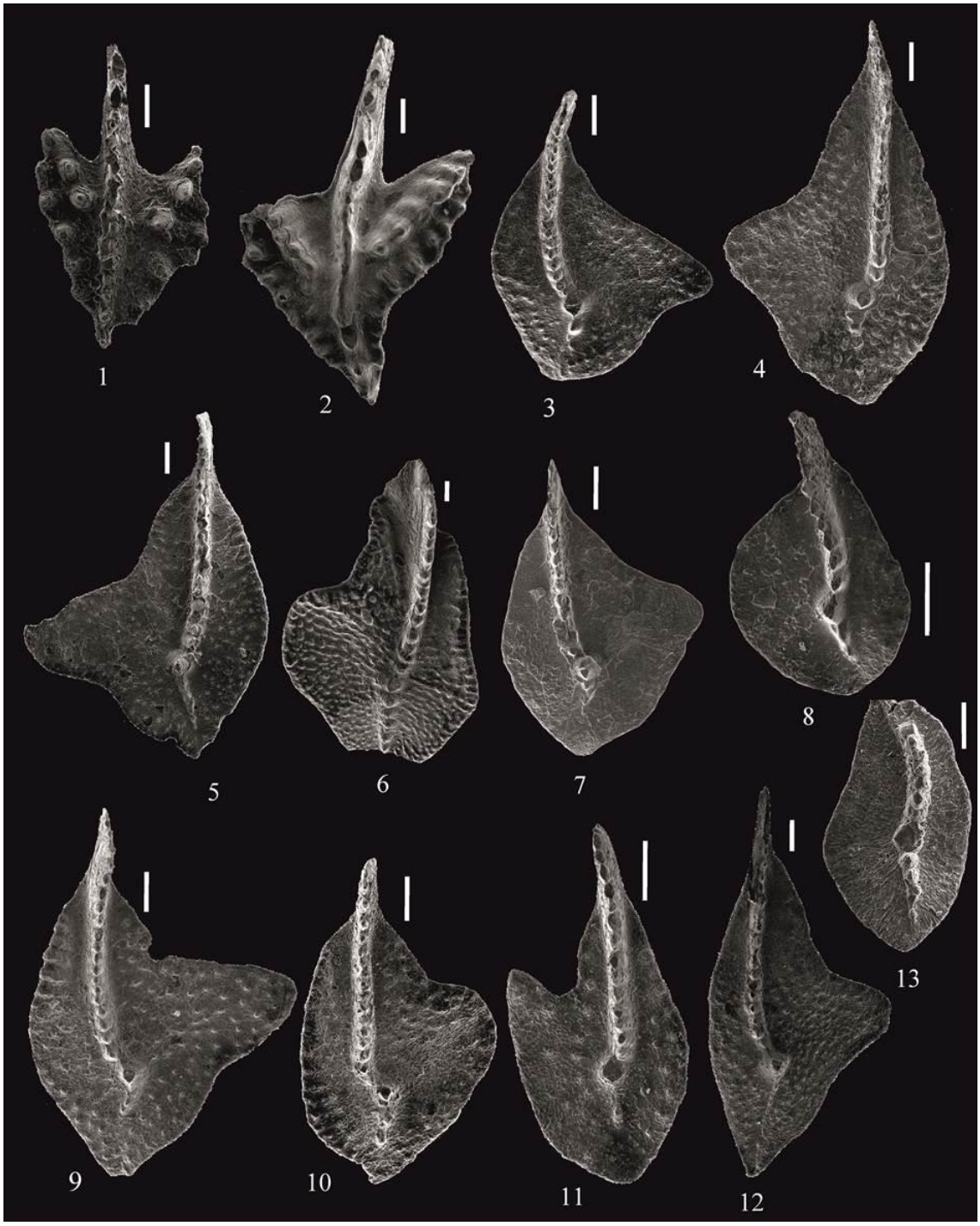

Figure 10. 1-2. *Ancyrodella nodosa* Ulrich and Bassler, 1926; (1) upper view of 492/24-12, sample 12; (2) upper view of 492/25-8, sample 14; **3.** *Palmatolepis* sp.; upper view of 492/24-5, sample 12; **4.** *Palmatolepis hassi* Müller and Müller, 1956; upper view of 492/24-7, sample 12; **5.** *Palmatolepis amplificata* Klapper, Kuzmin and

Ovnatanova 1996; upper view of 492/24-8, sample 12; **6.** *Palmatolepis domanicensis* Ovnatanova, 1976; upper view of 492/24-20, sample 13; **7.** *Palmatolepis lyaiolensis* Khruststcheva and Kuzmin, 1996; upper view of 492/24-4, sample 12; **8.** *Palmatolepis eureka* Ziegler and Sandberg, 1990; upper view of 492/25-17, sample 15; **9.** *Palmatolepis amplificata* Klapper, Kuzmin and Ovnatanova 1996; upper view of 492/25-7, sample 14; **10.** *Palmatolepis plana* Ziegler and Sandberg, 1990; upper view of 492/25-9, sample 14; **11.** *Palmatolepis* aff. *proversa* Ziegler, 1958; upper view of 492/25-6, sample 14; **12.** *Palmatolepis müelleri* Klapper and Foster, 1993; upper view of 492/25-26, sample 15; **13.** *Palmatolepis ederi* Ziegler and Sandberg, 1990; upper view of 492/26-15, sample 17. Scale bar is 0.1 mm.

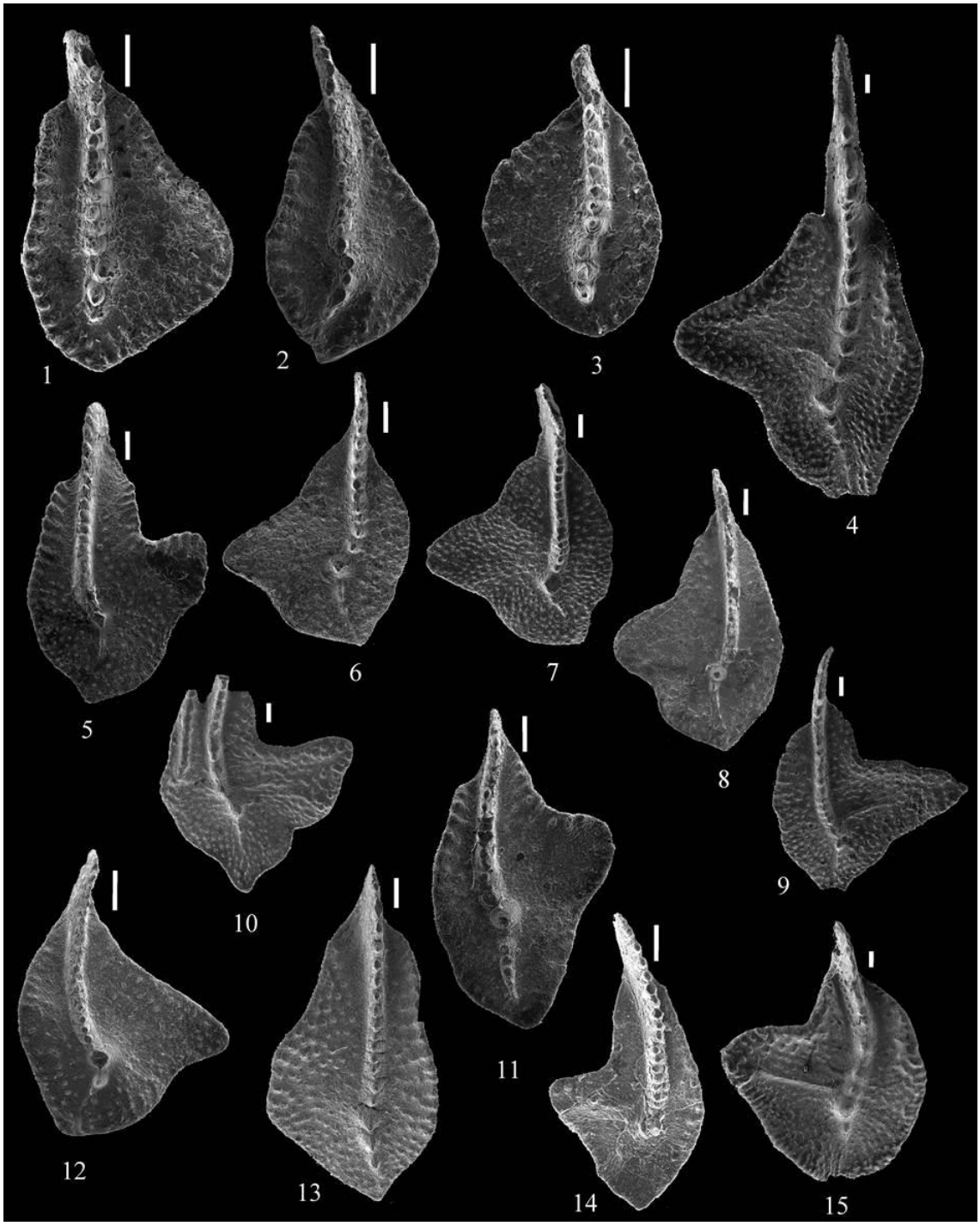

Figure 11. 1-2. *Palmatolepis foliacea* Youngquist, 1945; (1) upper view of 492/25-13, sample 15; (2) upper view of 492/26-12, sample 16; **3.** *Palmatolepis kozhimensis* Savage and Yudina, 2001; upper view of 492/25-11, sample 15; **4.** *Palmatolepis nasuta* Müller, 1956; upper view of 492/25-14, sample 15; **5, 10.** *Palmatolepis proversa*

Ziegler, 1958; (5) upper view of 492/25-20, sample 15; (10) upper view of 492/26-8, sample 16; **6-7.** *Palmatolepis* sp.; (6) upper view of 492/25-28, sample 15; (7) upper view of 492/26-18, sample 17; **8.** *Palmatolepis ljaschenkoae* Ovnatanova, 1976; upper view of 492/26-2, sample 15/2; **9.** *Palmatolepis brevis* Sandberg and Ziegler,1990; upper view of 492/25-29, sample 15; **11.** *Palmatolepis ormistoni* Klapper, Kuzmin and Ovnatanova, 1996; upper view of 492/26-13, sample 16; **12.** *Palmatolepis* sp.; upper view of 492/26-5, sample 16; **13.** *Palmatolepis* aff. *domanicensis* Ovnatanova, 1976; upper view of 492/26-7, sample 16; **14.** *Palmatolepis barba* Ziegler and Sandberg, 1990; upper view of 492/26-19, sample 17; **15.** *Palmatolepis bogartensis* (Stauffer, 1938); upper view of 492/26-6, sample 16. Scale bar is 0.1 mm.

Frasnian Zone (FZ)	1		2					3			4			5	11-12					13a	
Taxon/ Sample numb.	2	N4-2	3	N4-3	4	5/1	N4-5	5/2	5/3	6/1	7	8	N4-7	9/3	12	13	14	15	15/2	16	17
Ad. binodosa	2																				
Ad. pristina			3						1												
Ad. rotundiloba			1			1		1	1												
Ad. alata							3 aff.	4	2	1											
Ad. recta								5													
Ad. nodosa															1		5	2		1	
Ad. gigas															1			1 cf.			
Ad. ioides																				1	
Ancyrodella sp. indet.						2	3														
I. vitabilis	1							1													
I. symmetricus	2					2				1		1	1	3							
I. expansus	3								1												
I. obliquimarginatus	2																				
I. brevis				1																	
Icriodus sp. indet.	6		2		1	3			1		2	1		5		3 juv.	1	1		2	
P. varcus		1																			
P. parawebbi	1																				
P. latifossatus	1																				
P. pennatus	1		2		1	1	2 aff.				1										
P. dubius	1		1	1			1														
P. ljaschenkoi	1		2				2	1		1											
P. xylus	3		8		3	2								1							
P. decorosus	1				1		1			1	1				2	1	2	2		1	1
P. dengleri sagitta			5																		
P. dengleri dengleri			2																		
P. praepolitus			2		1				1												
P. webbi			1				1	1		1						1		2 aff.			
P. foliatus			3													1	1				
P. pseudoxylus			2						3					1			1				1
P. pollocki			1									2					1			1	
P. alatus			2					1													
P. paradecorosus									1												
P. aff. *brevilamiformis*													1								
P. timanicus														4							
P. uchtensis														6	1	1	7	19	1	3	
P. lodinensis														1		1	12	21		2	
P. mirificus																	3	2		1	
P. aequalis																	3				
Polygnathus sp. indet.	6		5		5	2	4	2	2		2	5		5			6	17	11	3	2
Polygnathus sp. indet. (juv.)			20							1					32		18	38		16	

Table 1. Distribution and number of conodonts found in the Matyashor Formation.

Frasnian Zone (FZ)	1		2					3			4			5	11-12					13a	
Taxon/ Sample numb.	2	N4-2	3	N4-3	4	5/1	N4-5	5/2	5/3	6/1	7	8	N4-7	9/3	12	13	14	15	15/2	16	17
Y. angustidiscus	1		2		1							1									
Youngquistognathus sp. indet.												1		1							
Belodella sp.		2		1			2														
Schmidthognathus sp.					1																
M. falsiovalis						2	2	1	1	1			2	3							
M. bogoslovskyi							1		1	1											
M. asymmetrica										1	1			2							
Mesotaxis sp. indet.														3							
Z. nuda						1				1											
Z. ovalis							1	1	1	1				3							
Zieglerina sp. indet.										1		1									
Mehlina gradata										1						1					
Pa. transitans											1	1 cf.		2							
Pa. ljaschenkoae															2		5	3	3	6	1
Pa. lyaiolensis															1						
Pa. hassi															1	1	2				
Pa. amplificata															1		1	1			
Pa. foliacea															1		1	2		4	
Pa. timanensis															1					1	
Pa. kireevae															1		8	1	1	3	1
Pa. plana																1	2	1			1 aff.
Pa. proversa																1	1 aff.	1		3	1
Pa. domanicensis																1	1			1 aff.	
Pa. jamieae savagie																	2				
Pa. nasuta																	1	1	2	1	
Pa. barba																		1		1	1
Pa. mülleri																		2			
Pa. mucronata																		1			
Pa. kozhimensis																		3		2	1
Pa. eureka																		1			
Pa. brevis																		2			
Pa. ormistoni																		1		1	
Pa. bogartensis (late form)																				1	
Pa. ederi																					2
Pa. aff. *jamieae*																					1
Palmatolepis sp. indet.													1	1	6		12	9	8	6	8
Palmatolepis sp. indet. (juv.)																4		32		21	
Ag. triangularis															2						
Ancyrognathus sp.															1 cf.			2			
total conodonts (sample)	32	3	64	3	14	16	23	18	16	13	8	13	5	41	54	17	96	158	26	82	21
total conodonts	723																				

Table 1 (continuation). Distribution and number of conodonts found in the Matyashor Formation.